Antiangiogenic Forms of Antithrombin Specifically Bind to the Anticoagulant Heparin Sequence[†]

Sophia Schedin-Weiss,*[,‡] Benjamin Richard,[§] Rebecka Hjelm,[‡] and Steven T. Olson[§]

Department of Medical Biochemistry and Microbiology, Uppsala University, Box 582, SE-751 23 Uppsala, Sweden, and Center for Molecular Biology of Oral Diseases, University of Illinois at Chicago, Chicago, Illinois 60612

Received August 31, 2008; Revised Manuscript Received November 7, 2008

ABSTRACT: A specific pentasaccharide sequence of heparin binds with high affinity to native antithrombin and induces a conformational change in the inhibitor by a previously described two-step interaction mechanism. In this work, the interactions of heparin with the antiangiogenic latent and cleaved antithrombin forms were studied. Binding of heparin to these antithrombin forms was specific for the same pentasaccharide sequence as native antithrombin. Rapid kinetic studies demonstrated that this pentasaccharide induced a conformational change also in latent and cleaved antithrombin. The binding affinities of these antithrombin forms for the pentasaccharide, as compared to native antithrombin, were ~30-fold lower due to two to three fewer ionic interactions, resulting in less stable conformationally altered states. Affinities of latent and cleaved antithrombin for longer heparin chains, containing the pentasaccharide sequence, were 2-fold lower than for the pentasaccharide itself. This contrasts the interaction with native antithrombin and demonstrates that residues flanking the pentasaccharide sequence of heparin are repelled by the latent and cleaved forms. These findings contribute to delineating the mechanism by which heparin or heparan sulfate mediates antiangiogenic activity of antithrombin.

The serpin, antithrombin, has been found to possess potent antiangiogenic properties in addition to being an important physiological anticoagulant. The anticoagulant native form of antithrombin has an intact surface-exposed loop, the reactive center loop (RCL),[1] containing a reactive site that is recognized by the target proteases. In contrast, the antiangiogenic activities are exerted by conformationally changed forms of the protein, i.e. cleaved, latent, and prelatent antithrombin (*1*−*5*). Cleaved antithrombin is formed by proteolytic cleavage in the RCL, which leads to the insertion of the N-terminal part of this loop as a new strand in the center of a large central β-sheet, called β-sheet A, of the inhibitor. Latent antithrombin is formed by mild heat treatment, which gives a conformation similar to cleaved antithrombin, although the RCL is intact. The latent and cleaved forms have lost their ability to inhibit proteases (*6, 7*). Prelatent antithrombin is formed as an intermediate in the conversion from native to latent antithrombin in the presence of stabilizing ions and possesses both anticoagulant and antiangiogenic properties (*3, 5*). The antiangiogenic forms of antithrombin have been found to inhibit angiogenesis in several *in vivo* models and to inhibit tumor growth in several mouse models (*1*−*3, 8*). Mechanisms of the antiangiogenic actions include inhibition of FGF-2 and VEGF-induced proliferation of endothelial cells (*2, 8*). Moreover, latent and cleaved antithrombin downregulate several proangiogenic genes and upregulate several antiangiogenic genes, suggesting that these antithrombin forms have direct signaling functions (*9*).

The interaction of heparin or heparan sulfate with native antithrombin plays an essential role in activating the inhibitory potential of antithrombin by increasing the rate of attack of the inhibitor on its target proteases, partially due to a bridging mechanism and partially due to an allosteric mechanism (*10*). In the bridging mechanism, protease−inhibitor complex formation is enhanced through the binding to the same heparin chain. The allosteric mechanism is achieved by a global conformational change, induced by the binding of a specific pentasaccharide sequence (*11*), and is accompanied by a 40% enhancement in tryptophan fluorescence (*12*). Heparin fractions that comprise this pentasaccharide sequence are denoted high-affinity heparin (HAH), and those that lack it are called low-affinity heparin (LAH).

It has recently been shown that the heparin-binding site is required for the antiangiogenic activities of latent and cleaved antithrombin, suggesting that heparin/heparan sulfate is involved in mediating these activities (*8*). An essential question is therefore whether the antiangiogenic antithrombin forms have different heparin sequence specificities than native antithrombin. In this work, the interactions of HAH, LAH, and two synthetic pentasaccharides with cleaved, latent, and native antithrombin were studied by fluorescence measurements and by an affinity matrix method. The heparin

[†] This work was supported by Swedish Research Council Grants 2003-6107 and 2005-6412 and by the Magnus Bergvall Foundation (to S.S.-W.) and by NIH grant HL-39888 (to S.T.O.).

* To whom correspondence should be addressed: phone, +46 18 4716655; fax, +46 18 4714673; e-mail, Sophia.Schedin_Weiss@imbim.uu.se.

[‡] Uppsala University.

[§] University of Illinois at Chicago.

[1] Abbreviations: AT, antithrombin; FGF, fibroblast growth factor; FGFR, FGF receptor; HAH, high-affinity heparin; LAH, low-affinity heparin; RCL, reactive center loop; SDS, sodium dodecyl sulfate; TNS, 2-(*p*-toluidinyl)naphthalene-6-sulfonic acid; VEGF, vascular endothelial growth factor; PAGE, polyacrylamide gel electrophoresis.

10.1021/bi801656u CCC: $40.75 © 2008 American Chemical Society
Published on Web 11/26/2008

preference of latent and cleaved antithrombin and the mechanism of heparin interactions with these antithrombin forms were characterized and compared with those of native antithrombin. Latent and cleaved antithrombins were found to have specificity for the same pentasaccharide sequence as native antithrombin, although with approximately 30-fold lower affinities. Furthermore, the interaction with longer heparin chains differed, because latent and cleaved antithrombin repelled heparin in what is in native antithrombin denoted the extended heparin-binding site. This information may be useful in defining the type of heparin or heparan sulfate that is used by the antiangiogenic antithrombin forms to mediate antiangiogenic activity. Moreover, since treatments with various heparin forms have been found to reduce the mortality rate of cancer (*13*), information on the sequences that interact with the different antithrombin forms may be of importance for achieving the optimal desired effects on angiogenesis as well as coagulation during such treatments.

EXPERIMENTAL PROCEDURES

Antithrombin Preparations. The α-form of antithrombin, i.e., the form that is glycosylated on all four potential N-glycosylation sites and constitutes ~90% of antithrombin in human blood (*14, 15*), was purified from human plasma as described previously (*16*). Latent antithrombin was prepared by incubating native antithrombin at 60 °C for 24 h in 10 mM Tris-HCl and 0.5 M sodium citrate and pH 7.4 (*2*). Human neutrophil elastase (Athens Research and Technology, Athens, GA) was used to cleave the RCL in native antithrombin to produce cleaved antithrombin, as described previously (*4, 17, 18*). SDS−PAGE and native PAGE, according to Laemmli, were used to assess the purity of the antithrombin variants (*16, 19*). The cleaved antithrombin variant was differentiated from native antithrombin by 10% SDS−PAGE under nonreducing conditions (*20*). The samples were boiled for 10 min before they were applied to the gel. Concentrations of the antithrombin variants were determined spectrophotometrically from the absorbance of 280 nm with the use of the molar absorption coefficient of 37700 M^{-1} cm^{-1} (*21*). The purified antithrombin forms were snap-frozen and stored at −70 °C. Native, latent, and cleaved antithrombins were >95% homogeneous in reducing SDS−PAGE, native PAGE, and nonreducing SDS−PAGE, respectively.

Heparins. The methyl α-glycoside form of the heparin pentasaccharide mimicking the antithrombin-binding site of heparin (Fondaparinux clinically used under the trade name Arixtra) (*22*) was a gift from Glaxo Smith Kline. This pentasaccharide is referred to as the normal pentasaccharide in this work. The monosaccharide units that it is composed of are denoted DEFGH from the nonreducing end. The synthetic O-methylated, O-sulfated pentasaccharide Idraparinux (*22*), here referred to as the high-affinity pentasaccharide, was supplied by Sanofi-Aventis. Heparins with low and high affinity for native antithrombin, i.e., lacking or containing the pentasaccharide and denoted LAH and HAH, respectively, with molecular weights of ~7900, were isolated as described previously (*16*).

Experimental Conditions. Equilibrium binding and kinetics of antithrombin−heparin interactions and thrombin inhibition stoichiometries were analyzed at 25 ± 0.2 or 10 ± 0.2 °C in 20 mM sodium phosphate buffer containing 0.1 mM EDTA and 0.1% polyethyleneglycol at pH 7.4. Sodium chloride was added to give the final ionic strength, which in most cases was 0.15, corresponding to physiological ionic strength.

Stoichiometries of Thrombin Inhibition. Stoichiometries of thrombin inhibition were determined as detailed previously (*16*). Briefly, an increasing amount of antithrombin was added to a fixed thrombin concentration of 0.5 μM in a final volume of 20 μL. Molar ratios of antithrombin/thrombin varied between 0 and 2. The mixture was incubated at 25 °C for at least 2 h, until complex formation was complete. Residual thrombin activity was determined by diluting the incubation mixture 1:200 into 110 μM thrombin substrate S-2238 (Haemochrom Diagnostica AB, Mölndal, Sweden). Substrate hydrolysis was recorded in a dual beam Hitachi U-2000 spectrophotometer at 405 nm. The residual thrombin activity was plotted against the molar ratio of antithrombin/thrombin, and the stoichiometry of inhibition was determined by linear regression from the abscissa intercept. Native antithrombin had a stoichiometry of inhibition indistinguishable from one, and latent and cleaved antithrombin were inactive.

Fluorescence Titrations. Equilibrium binding was studied by fluorescence titrations, monitored either by the tryptophan fluorescence change accompanying the interaction or by the fluorescence change obtained in the presence of a fluorescent probe, TNS (Invitrogen). TNS binds weakly to antithrombin, and the fluorescence of the TNS-bound antithrombin complex decreases upon heparin binding (*23*), which is useful for assessing certain antithrombin−heparin interactions that are not accompanied by changes in tryptophan fluorescence. The change in TNS-bound antithrombin fluorescence induced by heparin binding was experimentally more difficult to determine than the tryptophan fluorescence, because we found that (i) the TNS−antithrombin fluorescence decreased exponentially with time during the first hour after mixing, presumably due to a slow isomerization of the bound probe, and (ii) high heparin concentrations caused a fluorescence change with TNS even in the absence of antithrombin. TNS fluorescence was thus the optimal choice mainly for studies of the interactions of pentasaccharide and HAH with cleaved antithrombin, as the binding of the two saccharides to latent antithrombin caused a larger tryptophan but smaller TNS fluorescence change than the binding to cleaved antithrombin. In other cases tryptophan fluorescence was the preferred method. In TNS titrations, antithrombin and TNS were mixed 30−45 min before the titration, and the titrations were subtracted by blank titrations of buffer into TNS-bound antithrombin. Heparin concentrations used in these titrations minimally affected the reported changes in TNS fluorescence. The titrations were done in an SLM 4800S spectrofluorometer (SLM instruments, Rochester, NY). Excitation and emission wavelengths of 280 and 336−340 nm, respectively, and excitation and emission bandwidths of 2 and 16 nm, respectively, were used for tryptophan fluorescence measurements. For TNS titrations, excitation and emission wavelengths were 326 and 455 nm, and excitation and emission bandwidths were 4 and 16 nm, respectively.

Stoichiometric titrations for the binding of pentasaccharide to latent antithrombin were done at 20 μM antithrombin and were based on the tryptophan fluorescence change. Affinity

titrations, based on either tryptophan or TNS fluorescence change, were done at 100−500 nM native antithrombin or 0.5−5 μM latent and cleaved antithrombin. The titrations in the presence of TNS were usually conducted in 10−20 μM and, in some cases, 40 μM TNS. Binding stoichiometries and dissociation equilibrium constants, K_D, were determined by fitting the data to the equilibrium binding equation by nonlinear least-squares analysis, as described before (*16*). The ionic strength dependence for the interactions between the saccharides and the antithrombin forms was determined by measuring K_D values at different sodium ion concentrations, as described previously (*24*).

TNS Fluorescence Spectra. The effects of the interactions of the normal pentasaccharide, LAH, and HAH with the antithrombin forms on the fluorescence of AT-bound TNS were determined from emission spectra measured from λ_{em} 380 to 530 nm at λ_{ex} 326 nm. The excitation and emission bandwidths were 5 and 3 nm, respectively. Spectra were run for free TNS, TNS plus the heparin forms, TNS plus the antithrombin variants, and TNS plus the antithrombin variants plus the heparin forms. The fluorescence change at 455 nm induced by heparin was expressed relative to that of the antithrombin-bound TNS after subtraction of the effect of heparin on the fluorescence of free TNS.

Rapid Kinetics of Pentasaccharide Binding to the Antithrombin Forms. Rapid kinetics of normal pentasaccharide binding to native and latent antithrombin were measured by monitoring the change in tryptophan fluorescence accompanying the interaction in an SX-17MV stopped-flow instrument (Applied Photophysics, Leatherhead, U.K.), essentially as described previously (*25*), at λ_{ex} 280 nm and with the use of a 330 nm emission bandpass filter. The experiments were conducted at ionic strength 0.15, pH 7.4, and 10 °C. The low temperature was introduced to enhance the small fluorescence signal for the interaction of the pentasaccharide with latent antithrombin. Kinetics for normal pentasaccharide binding to cleaved antithrombin was monitored under the same conditions as the binding to native and latent antithrombin, except that the change in TNS fluorescence, monitored at λ_{ex} 326 nm and with an emission 420 nm cutoff filter, was analyzed. No background TNS fluorescence change was observed under these conditions during the time frame of the fluorescence traces. Pseudo-first-order conditions were arranged, with the pentasaccharide concentration in at least a 5-fold, and in most cases a 10-fold, ratio to the protein concentration. Observed pseudo-first-order rate constants, k_{obs}, were obtained by least-squares fitting of the fluorescence traces to a single-exponential function by nonlinear regression. Each k_{obs} value reported represents the average ± SEM of 16−37 traces.

Affinity Matrix Interaction Studies. Interactions of the normal pentasaccharide, LAH, and HAH with the antithrombin forms were further studied by an affinity matrix method detailed previously (*26*). This method is based on the binding of the antithrombin forms to a heparin matrix (heparin−Sepharose) and the displacement of antithrombin from the matrix by heparin competitors. Control binding experiments were first done by measuring the amount of antithrombin bound to the matrix as a function of the total antithrombin concentration. To this end, increasing concentrations of each antithrombin form were incubated during shaking in the presence (or absence for unbound control) of 50 μL of heparin−Sepharose in 500 μL final volume for 2 h at room temperature. The samples were then centrifuged, and antithrombin concentration in the supernatant was determined. Competitive binding experiments were conducted similarly but with a fixed antithrombin concentration of 200 nM and increasing concentrations of heparin forms. The unbound antithrombin concentration was determined by fluorescence measurements at λ_{ex} 280 nm and λ_{em} 340 nm after addition of 3 M NaCl and Polybrene to the supernatant to avoid heparin effects on the antithrombin fluorescence. Fluorescence values were corrected for the dilution. The following equation was used for fitting the displacement data (*26*):

$$[A]_{b,X} = C3([A]_T - [A]_{b,B}) \quad (1)$$

where

$$[A]_{b,B} = 0.5\{([A]_T + n[B]_T + K_{AB}/(1 - C3)) - \sqrt{(([A]_T + n[B]_T + K_{AB}/(1 - C3))^2 - 4n[B]_T[A]_T)}\}$$

In this equation A is antithrombin, B is heparin competitor, $[A]_T$ and $[B]_T$ represent total concentrations of A and B, n is the stoichiometry of the competitor interaction, K_{AB} is the K_D for antithrombin binding to competitor heparin in solution, and C3 is the slope of the control curve for binding of antithrombin to the matrix. $[A]_{b,X}$ is the concentration of antithrombin bound to the matrix, and $[A]_{b,B}$, i.e., the concentration of antithrombin bound to the heparin competitor, is given above. C3 was used as a fitted parameter to avoid the effects of different binding efficiencies between different experiments. A stoichiometry, n, of 1 was assumed for all interactions.

RESULTS

Changes in Tryptophan and TNS Fluorescence Induced by the Interactions of Heparins with the Antithrombin Forms. The different heparin saccharides were titrated into a solution of protein or protein−TNS, and the resulting change in tryptophan or TNS fluorescence was monitored. The titrations were conducted up to saccharide concentrations at which saturation of the proteins was approached. The data were fit well by the equilibrium binding equation, as shown for the interactions of HAH with the antithrombin forms in Figure 1. The changes in tryptophan fluorescence for the binding of the saccharides to latent antithrombin at saturation were considerably smaller than for the binding to native antithrombin (Table 1). Even smaller changes in tryptophan fluorescence were observed for the binding of the saccharides to cleaved antithrombin. Of all the saccharides, LAH caused the smallest tryptophan fluorescence change for the binding to all antithrombin forms.

TNS has previously been used to study certain protein−heparin interactions when the tryptophan fluorescence change is limited (*8, 23, 27*). Titrating heparin into TNS-bound native antithrombin has previously been shown to result in a decrease of TNS fluorescence (*23*). Such a decrease was also observed in this work on HAH or pentasaccharide binding to all antithrombin forms studied. In contrast, LAH caused no measurable change in TNS fluorescence, either with native, latent, or cleaved antithrombin (Table 1). This low or absent fluorescence change indicates that LAH binds in a different mode than HAH or the pentasaccharides to all of

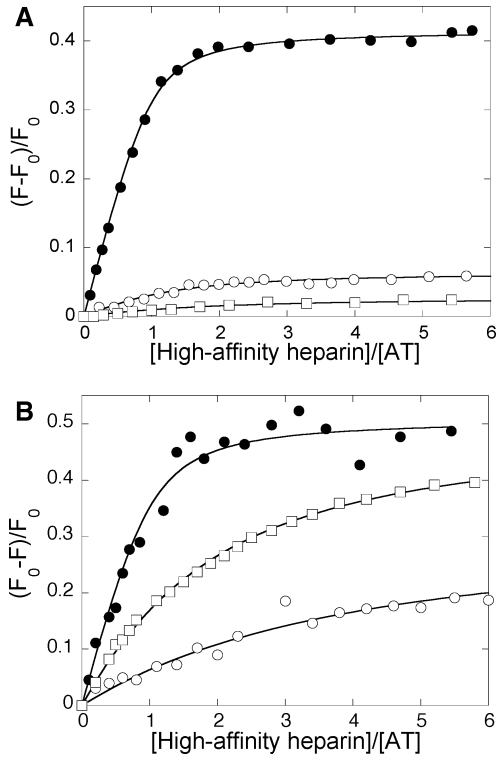

FIGURE 1: Equilibrium binding, studied by fluorescence titrations, for the interactions of high-affinity heparin with native, latent, and cleaved antithrombin. The changes in tryptophan fluorescence are shown for the interactions of high-affinity heparin with native, latent, and cleaved antithrombin (A) and the changes in TNS fluorescence for the interactions of high-affinity heparin with native, latent, and cleaved antithrombin (B). The protein concentrations used for the titrations were 0.5 μM native antithrombin, 3.5 μM latent antithrombin, and 2 μM cleaved antithrombin in (A) and 0.2 μM native antithrombin, 1 μM latent antithrombin, and 1.8 μM cleaved antithrombin in (B). Key: ●, native antithrombin; ○, latent antithrombin; □, cleaved antithrombin.

Table 1: Changes in Tryptophan and TNS Fluorescence Obtained by LAH, HAH, and Normal Pentasaccharide Binding to Native, Latent, and Cleaved Antithrombin (AT)[a]

AT form	fluorescence form	fluorescence change (%)		
		normal pentasaccharide	HAH	LAH
native	tryptophan	40	43	8
	TNS	28	51	0
latent	tryptophan	6	6	2
	TNS	24	32	0
cleaved	tryptophan	3	3	<1
	TNS	66	51	0

[a] The changes in tryptophan fluorescence were obtained from the ΔF_{max} values derived from computer fits of stoichiometric titration data to the equilibrium binding equation. The changes in TNS fluorescence were obtained from emission spectra recorded at λ_{ex} 326 nm, as described in Experimental Procedures. The negative changes in TNS fluorescence values at λ_{em} 455 nm are reported.

these antithrombin forms, as described previously for native antithrombin (*28*). A different binding mode may result from LAH inducing more limited conformational changes in latent and cleaved antithrombins.

Binding Affinities Determined by Fluorescence. Dissociation equilibrium constants, K_D, for the interactions between the saccharides and the antithrombin forms were determined by fluorescence titrations (Table 2). Titration data were computer-fit to the spectroscopic equilibrium binding equation (*16*). Equimolar binding stoichiometries have previously been reported for the binding of the normal pentasaccharide, the high-affinity pentasaccharide, HAH, and LAH to native antithrombin and for the binding of HAH and the high-affinity pentasaccharide to cleaved antithrombin (*7, 8, 29, 30*). We similarly determined a 1:1 stoichiometry for the binding of the normal pentasaccharide to latent antithrombin. For the remaining saccharide−antithrombin interactions, 1:1 stoichiometries were assumed. Native and latent antithrombins were titrated with the normal pentasaccharide in experiments monitored by both tryptophan and TNS fluorescence, which gave similar K_D values (Table 2). The K_D value for the binding of the normal pentasaccharide to native antithrombin, 50 nM, is in agreement with previous studies (*31*). Affinities of the normal pentasaccharide for latent and cleaved antithrombin were 30-fold lower than those for native antithrombin (Table 2), whereas the affinities of the high-affinity pentasaccharide for latent antithrombin was over 100-fold lower and for cleaved antithrombin about 40-fold lower than for the native protein. The affinities of the normal pentasaccharide were up to 2-fold higher than those of HAH for latent and cleaved antithrombin, even though high-affinity heparin contains the pentasaccharide sequence. No K_D values could be obtained from the low or absent fluorescence changes observed on binding of LAH to latent and cleaved antithrombin, either in the presence or in the absence of TNS. In two previous studies up to 10-fold higher K_D values have been reported for the interactions of pentasacharide or HAH with latent and cleaved antithrombin (*7, 32*). Our values were, however, verified by three different techniques, including the more sensitive TNS-binding assay, and a more recent study reported K_D values similar to those presented here for pentasaccharide interactions with latent and cleaved antithrombin (*8*).

Table 2: Dissociation Equilibrium Constants, Determined by Fluorescence Titrations, for the Interactions of Pentasaccharides and HAH with the Antithrombin Forms at 25 °C, pH 7.4, and Ionic Strength 0.15[a]

heparin form	antithrombin form	K_D (nM)
normal pentasaccharide	native	50 ± 3^b
		45 ± 7^c
	latent	1700 ± 200^b
		1200 ± 200^c
	cleaved	1400 ± 200^c
high-affinity pentasaccharide	native	$0.4 \pm 0.1^{b,d}$
	latent	70 ± 4^b
	cleaved	15 ± 1.3^c
HAH	native	32 ± 10^b
	latent	4400 ± 800^b
		2400 ± 500^c
	cleaved	1800 ± 90^c

[a] Dissociation equilibrium constants were determined by fluorescence titrations, monitored by tryptophan or TNS fluorescence, as described in Experimental Procedures. The values are the means ± SE of at least three titrations. [b] Titrations were based on the change in tryptophan fluorescence. [c] Titrations were based on the change in TNS fluorescence. [d] The value was calculated from the linear dependence of log K_D on log Na^+.

Ionic and Nonionic Contributions to the Affinity. The ionic and nonionic contributions to the interactions between the pentasaccharides and the antithrombin forms were determined from the dependence of log K_D on log [Na^+], as described before (*24, 30, 33*) (Figure 2). The normal pentasaccharide binds to native antithrombin with ~4 ionic interactions and a nonionic K_D value of 63 μM (*34*). Whereas

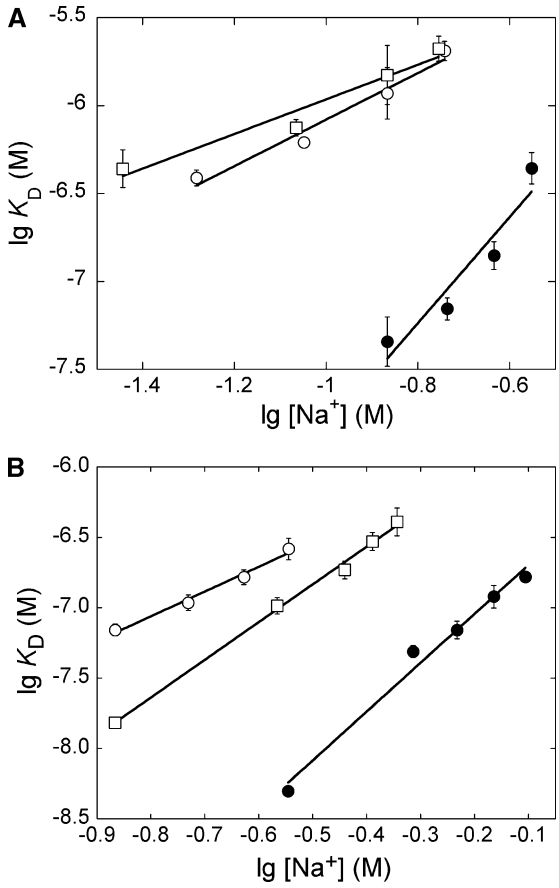

FIGURE 2: Double-logarithmic plots of the dependence of the K_D on [NaCl] for the binding of different heparins to native, latent, and cleaved antithrombin. K_D values were determined by fluorescence titrations at different sodium ion concentrations for the binding of normal pentasaccharide (A) or high-affinity pentasaccharide (B) to native antithrombin (●), latent antithrombin (○), and cleaved antithrombin (□). The ionic and nonionic contributions to the interactions were obtained as described in Experimental Procedures. The titrations in panel A and those of cleaved antithrombin in panel B were based on TNS fluorescence, whereas all other titrations were based on tryptophan fluorescence. The values are the means ± SE of two to four titrations. Error bars that are not shown are hidden by the symbols.

the high-affinity pentasaccharide also binds to native antithrombin with ~4 ionic interactions, the nonionic K_D value is considerably lower, 0.45 μM (*35*). Binding of the normal pentasaccharide to latent and cleaved antithrombin was shown to involve two to three less ionic interactions than the binding to native antithrombin, whereas the nonionic affinity was similar (Table 3). The binding of the high-affinity pentasaccharide to latent antithrombin similarly involved two less ionic interactions than the binding to native antithrombin. However, the interaction of the high-affinity pentasaccharide with cleaved antithrombin involved only one less ionic interaction compared with native antithrombin, demonstrating a somewhat different binding mode of this pentasaccharide to cleaved than to latent antithrombin. In contrast to normal pentasaccharide binding, the nonionic affinity was lower (5−10-fold) for the binding of the high-affinity pentasaccharide to latent and cleaved antithrombin than for the binding to the native protein.

Rapid Kinetics of Pentasaccharide Binding. The kinetics for the interactions of the normal pentasaccharide with native, latent, and cleaved antithrombin were determined from the

Table 3: Ionic and Nonionic Contributions to the Interactions of Pentasaccharides with Native and Latent Antithrombin at 25 °C and pH 7.4[a]

pentasaccharide	antithrombin form	Z	K_D' (μM)
normal pentasaccharide	native	4.4 ± 0.3[b]	63 ± 30[b]
	native	3.8 ± 0.9[c]	15 ± 17[c]
	latent	1.7 ± 0.2[c]	18 ± 7[c]
	cleaved	1.2 ± 0.2[c]	10 ± 4[c]
high-affinity pentasaccharide	native	4.3 ± 0.3[d]	0.45 ± 0.08[d]
	latent	2.2 ± 0.2	2.2 ± 0.5
	cleaved	3.3 ± 0.1[c]	3.2 ± 0.4[c]

[a] The number of ionic interactions, Z, and the nonionic affinities, K_D', were determined from the slopes and y-intercepts, respectively, of double-logarithmic plots of K_D versus [Na^+] (Figure 2). The slopes and intercepts ± SE were obtained by linear regression. [b] Taken from ref *34*. [c] Titrations were done in the presence of TNS. [d] Taken from ref *35*.

change in tryptophan or, in the case of the cleaved form, TNS fluorescence, under pseudo-first-order conditions at 10 °C. This low temperature was used because it was experimentally found to give fluorescence traces with improved signal-to-noise ratio than at 25 °C for the interaction of the pentasaccharide with latent antithrombin, for which the fluorescence change at saturation is only ~6% (Table 1). This improvement is presumably, at least partially, due to the ~10-fold increase in affinity at this temperature (Table 4), resulting in a larger proportion of antithrombin−pentasaccharide complex at equilibrium. Observed pseudo-first-order rate constants, k_{obs}, were determined at different pentasaccharide concentrations. In the low concentration range, 0−0.3 μM, the dependences of k_{obs} on the pentasaccharide concentration were essentially linear for native and latent antithrombin (Figure 3A), giving the bimolecular association rate constants, k_{on}, from the slope and the dissociation rate constants, k_{off}, from the y-intercept (Table 4). In the case of cleaved antithrombin, the analyses by TNS fluorescence did not give sufficiently reproducible k_{obs} values in the low pentasaccharide concentration range to allow determination of k_{on} and k_{off}. For native antithrombin, k_{on} at 10 °C was similar to the values obtained previously at 25 °C whereas k_{off} at 10 °C was approximately 15-fold lower (*30, 34*) (Table 4). There was no observable difference in k_{on} for the interactions of the pentasaccharide with latent and native antithrombin at 10 °C (30 ± 4 and 33 ± 1 M^{-1} s^{-1}, respectively), whereas k_{off} was substantially higher for the interaction with latent than for that with native antithrombin (1.5 ± 0.9 and 0.1 ± 0.2 s^{-1}, respectively) (Table 4).

The dependence of k_{obs} for the interactions with native, latent, and cleaved antithrombin on the pentasaccharide concentration was extended to higher such concentrations. The resulting curves were hyperbolic and could be well fit to the rectangular hyperbolic equation described previously (*30, 36*) (Figure 3B). This behavior indicates that the interactions of the pentasaccharide with latent and cleaved antithrombin are accompanied by a conformational change, similarly to native antithrombin (*30*), according to the two-step mechanism described in Scheme 1.

In this scheme, H is HAH or pentasaccharide, K_1 is the dissociation equilibrium constant for the first binding step, k_{+2} is the forward rate constant for the second, conformational change step, and k_{-2} is the reverse rate constant for the second binding step. The absence of any detectable lag

Table 4: Kinetic and Dissociation Equilibrium Constants for the Interactions of the Normal Pentasaccharide with Native, Latent, and Cleaved Antithrombin at 10 °C, Ionic Strength 0.15, and pH 7.4[a]

antithrombin form	k_{on} (10^6 M^{-1} s^{-1})	k_{off} (s^{-1})	k_{-2} (s^{-1})	K_1 (μM)	k_{+2} (s^{-1})	K_d (nM)
native	33 ± 1	0.1 ± 0.2	0.3 ± 0.9	6 ± 0.4	200 ± 5	4 ± 2
latent	30 ± 4	1.5 ± 0.9	3 ± 1	9 ± 1	200 ± 15	150 ± 50
cleaved	14 ± 6[b]	2 ± 2[c]	9 ± 2	14 ± 4	200 ± 30	160 ± 90

[a] Kinetic constants were determined by stopped-flow fluorometry, monitoring the change in tryptophan or TNS fluorescence induced by pentasaccharide binding, as described in Experimental Procedures. k_{on} and k_{off} were determined form the slopes and ordinate intercepts of linear plots of observed pseudo-first-order rate constants, k_{obs}, versus pentasaccharide concentration (Figure 3A). k_{on} and k_{off} values ± SE were calculated by linear regression. K_1, k_{+2}, and k_{-2} were determined by fitting the data from the plots of Figure 3B to the rectangular hyperbolic equation (*36*). These values ± SE were calculated by nonlinear regression. K_D values are the means ± SE of three fluorescence titrations conducted at 10 °C as described in Experimental Procedures. [b] Calculated from K_1 and k_{+2}. [c] Calculated from K_1, k_{+2}, and K_D.

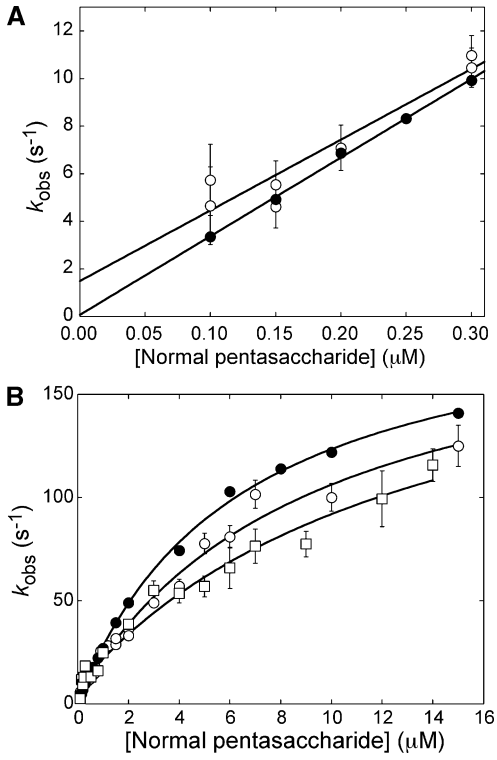

FIGURE 3: Rapid kinetics for the interactions of the normal pentasaccharide with native, latent, and cleaved antithrombin. Observed rate constants, k_{obs}, were determined under pseudo-first-order conditions at 10 °C, ionic strength 0.15, and pH 7.4 in the low (A) and high (B) concentration ranges, as described in Experimental Procedures. Each k_{obs} value represents the average of 16−37 fluorescence traces. Key: ●, native antithrombin; ○, latent antithrombin; □, cleaved antithrombin.

Scheme 1

$$\mathrm{AT + H} \underset{}{\overset{K_1}{\rightleftharpoons}} \mathrm{AT\text{-}H} \underset{k_{-2}}{\overset{k_{+2}}{\rightleftharpoons}} \mathrm{AT^{*}\text{-}H}$$

phase for the interaction of the pentasaccharide with latent and cleaved antithrombin over the pentasaccharide concentration range studied is in agreement with a rapid equilibrium being established in the first binding step, as described previously for the interactions of HAH and pentasaccharide with native antithrombin at 25 °C (*30, 36*). The kinetic constants characterizing the two-step mechanism for pentasaccharide binding to native antithrombin at 10 °C differed from those determined previously at 25 °C. The K_1 and k_{+2} values were 6 ± 0.5 μM and 200 ± 5 s^{-1} at 10 °C, compared with 22 ± 2 μM and 750 ± 50 s^{-1} at 25 °C (*34*). The first binding step is thus 3−4-fold tighter, whereas the forward rate constant of the second binding step is 3-fold lower at the lower temperature. K_1 was somewhat higher for the interaction of the pentasaccharide with latent antithrombin and twice as high for the interaction with cleaved antithrombin than for that with native antithrombin, whereas k_{+2} was indistinguishable for the interactions of the pentasaccharide with the three antithrombin forms (Table 4). For cleaved antithrombin, the experimentally determined values of K_1 and k_{+2} were used to calculate k_{on} and subsequently k_{off}. Although there was a small decrease in k_{on}, the values show that the major factor causing the decreased affinity of the normal pentasaccharide for cleaved than for native antithrombin was a substantial increase in k_{off}, as in the case of latent antithrombin.

Affinity Matrix Results. Due to the inadequacy of fluorescence techniques for quantifying the interactions of LAH with latent and cleaved antithrombin, an affinity matrix method was additionally used (*26*). Control experiments verified that the amount of antithrombin bound to the heparin−Sepharose gel increased linearly with the total antithrombin concentration up to 500 nM for the three antithrombin forms (Figure 4A). Under such linear conditions, the equation used for fitting the binding data in the presence of heparin competitor reduces to a quadratic equation (eq 1) (*26*). In the absence of heparin competitor, more native than latent or cleaved antithrombin bound to the matrix, as expected from the affinity difference (Figure 4A). Furthermore, less latent than cleaved antithrombin was bound, in agreement with affinities determined by fluorescence titrations (Table 2).

Heparin competitors caused the displacement of bound antithrombin from the matrix in a concentration-dependent manner (Figure 4B−D). The data for the binding of all heparin forms to all three antithrombin variants were readily fit by eq 1 (solid lines of Figure 4B−D), confirming that all heparin forms bind to the same or overlapping sites of all antithrombin forms, which has previously been shown only for native antithrombin (*28, 37*). Affinities obtained by analysis of the binding of the three types of heparin to the three antithrombin forms are shown in Table 5. K_D values were difficult to determine for competitor heparin interactions in cases where antithrombin was tightly bound to the matrix, as for native antithrombin, due to the large excess of antithrombin-binding sites on the matrix and, thus, low amount of unbound antithrombin. This resulted in large errors in the K_D values and deviation from the values obtained by fluorescence titrations. In contrast, the K_D values for the interactions of the normal pentasaccharide and HAH with latent and cleaved antithrombin were well determined and similar to the values obtained by fluorescence titrations

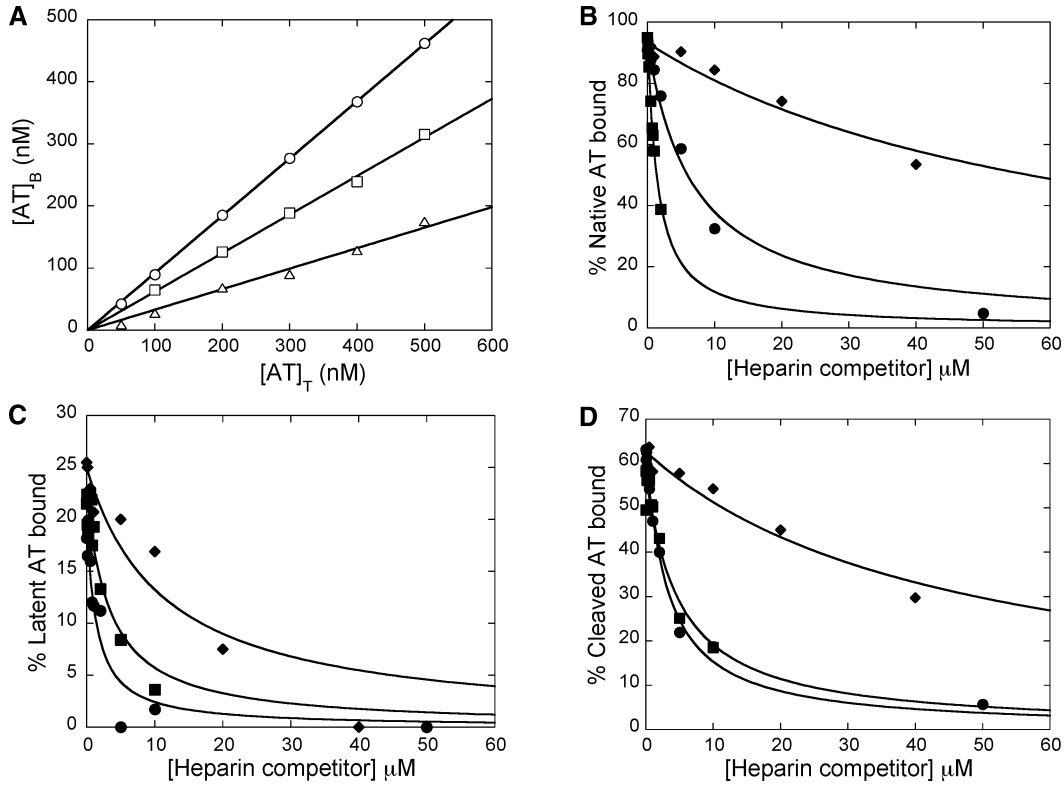

FIGURE 4: Binding of native, latent, and cleaved antithrombin to a heparin matrix in the absence or presence of heparin competitors. Binding was first studied as a function of increasing total antithrombin concentrations in the absence of heparin competitors (A). The displacement of antithrombin by increasing amounts of heparin competitors was then analyzed for native (B), latent (C), and cleaved (D) antithrombin forms. The solid line in (A) represents linear regression fitting. The solid lines in (B−D) represent nonlinear regression fitting to eq 1, as described in Experimental Procedures. Key: ○, native antithrombin; □, cleaved antithrombin; △, latent antithrombin; ◆, LAH; ■, HAH; ●, normal pentasaccharide.

Table 5: Dissociation Equilibrium Constants Determined by the Affinity Matrix Method for the Interactions of the Normal Pentasaccharide and High- and Low-Affinity Heparins with Native, Latent, and Cleaved Antithrombin[a]

	K_D (nM)		
heparin form	native AT	latent AT	cleaved AT
normal pentasaccharide	450 ± 160	1100 ± 350	1200 ± 120
HAH	59 ± 10	2700 ± 730	2100 ± 400
LAH	4400 ± 1500	8400 ± 2900	17000 ± 2700

[a] The antithrombin forms were bound to a heparin−Sepharose matrix, and the displacement from this matrix by increasing pentasaccharide or heparin concentrations was analyzed, as described in Experimental Procedures. 26 saccharide heparins were used. K_D values ± SE were determined by nonlinear regression of the binding data of Figure 4B−D to eq 1.

(Table 2), verifying the validity of this method. These values also confirmed the finding obtained by fluorescence titrations that the pentasaccharide binds with approximately 2-fold higher affinities than HAH to latent and cleaved antithrombin. With this method the affinities of LAH for latent and cleaved antithrombin could also be determined and were clearly found to be weaker than the affinities of the normal pentasaccharide and HAH for these antithrombin forms. However, the difference in affinities of low- and high-affinity heparins for latent and cleaved antithrombin was considerably smaller than the 1000-fold difference in affinity of the two heparin forms for native antithrombin (*28, 29*).

DISCUSSION

In this study we have characterized the interactions of various heparin and pentasaccharide forms with latent and cleaved antithrombin. Rapid kinetic experiments provided evidence for a similar two-step mechanism for the interaction of the normal pentasaccharide with latent and cleaved as with native antithrombin, i.e., an initial weak interaction followed by a conformational change. The considerably lower tryptophan fluorescence changes observed in this study for normal pentasaccharide binding to latent and cleaved than to native antithrombin reflect that the latent and cleaved forms were unable to undergo the same pentasaccharide-induced conformational change as native antithrombin. This finding is strengthened by the crystal structure of pentasaccharide-bound native and latent antithrombins (*38*) (Figure 5), which reveals for instance that pentasaccharide binding induces the formation of a 1.5 turn α-helix, called the P-helix, in both antithrombin forms. In contrast, the pentasaccharide-induced 2-turn elongation of the D-helix and the expulsion of the RCL from sheet A occur in native but not in latent antithrombin.

The 20−30-fold lower affinities of the normal pentasaccharide for latent and cleaved than for native antithrombin were fully accounted for by two and three less ionic interactions, respectively, whereas the nonionic contributions to the binding were essentially the same. The decreased affinity was almost completely due to a decrease in k_{off}, whereas K_1 was only slightly decreased and k_{+2} was unchanged. As k_{+2} values for heparin−antithrombin interactions are independent of ionic strength (*30, 35, 36*), these findings imply that all of the ionic interactions for the binding of the normal pentasaccharide to latent and cleaved antithrombin are made in the first binding step. In fact, the

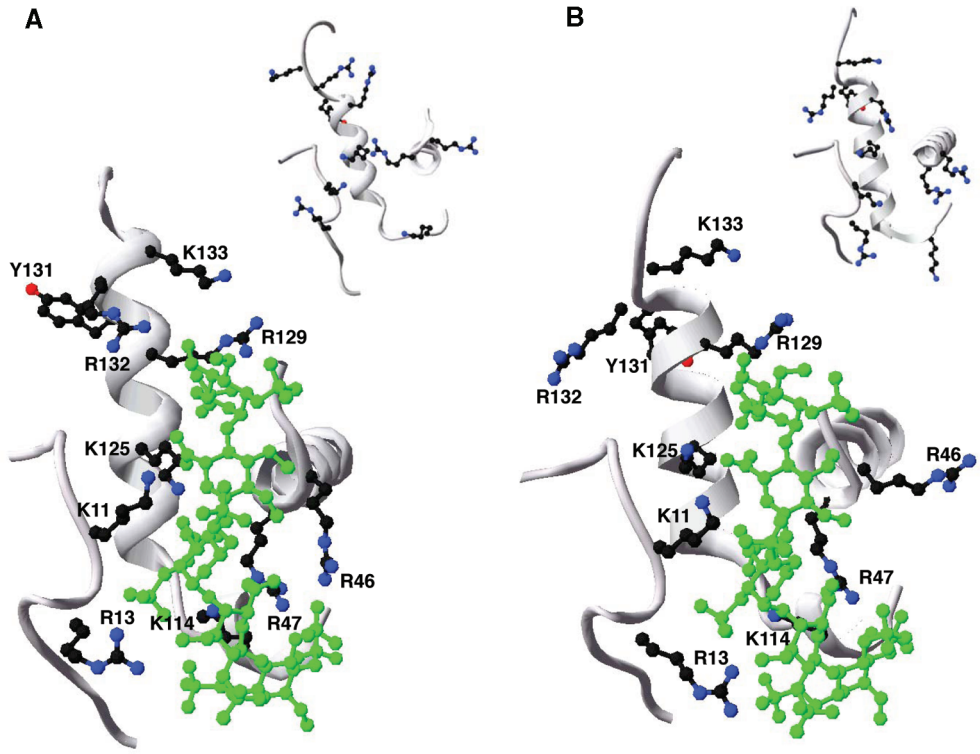

FIGURE 5: Close-up of the pentasaccharide-binding site of native and latent antithrombin forms. The image shows a close-up of the D- and P-helices and parts of the N-terminal region and the A-helix of the heparin-binding site of native antithrombin (A) and latent antithrombin (B) in complex with a high-affinity pentasaccharide (large pictures; PDB code 1e03) and in the unbound state (inset pictures; PDB code 1e05). A ribbon presentation of the selected parts of the protein backbone is shown in gray. The amino acid side chains of the residues of the N-terminus and the A-, D-, and P-helices that are known to participate in the interaction of pentasaccharide with native antithrombin are shown. Additionally, the amino acid side chains of Arg132 and Lys133, forming part of the extended heparin-binding site of native antithrombin, and Tyr131, are shown. Carbon atoms of amino acid side chains are drawn in black, nitrogen atoms in blue, and oxygen atoms in red. The pentasaccharide is drawn in green. The images were produced in Swiss PDB viewer.

number of ionic interactions made in the first step of the normal pentasaccharide binding to native antithrombin is similar to what was observed here for the overall interaction of this pentasaccharide with latent and cleaved antithrombin. The higher k_{off} for the interaction of the pentasaccharide with latent and cleaved antithrombin thus appears to result from only nonionic interactions, without any ionic contributions, being established in the conformational activation step. N−O binding distances between Arg129, Lys125, and Arg46 and the interacting functional groups of the pentasacharide in PDB structure 1e03 were longer in latent than in native antithrombin, which may explain the reduced number of ionic interactions in the pentasaccharide-bound latent form. The formation of salt bridges between these residues of active antithrombin and the normal pentasaccharide has been verified in the antithrombin−S195A factor Xa−pentasaccharide complex structure (*39*). The lower extent of pentasaccharide-induced changes in the positions of the pentasaccharide-binding basic residues in latent than in native antithrombin (Figure 5) thus appears to be due to a reduced number of ionic interactions stabilizing the activated state. Previous studies have suggested that D-helix elongation is important for the allosteric activation of native antithrombin (*40, 41*). Interestingly, a Lys133Pro antithrombin variant, whose D-helix cannot be elongated, binds the normal pentasaccharide with similar affinity and kinetics as latent and cleaved antithrombin (*40*). The compaction of the structure that forces the expulsion of the RCL in native antithrombin is likely driven by exposure of Tyr131 when helix D extends (*41*). In contrast to native antithrombin, Tyr131 is identically positioned in the free and pentasaccharide-bound forms of latent antithrombin (Figure 5). Together, these findings suggest that activated antithrombin has higher affinity for the pentasaccharide than antithrombin forms incapable of extending their D helix, due to the greater number of ionic interactions being made in the activated state (*30, 34*).

The limited fluorescence changes observed when pentasaccharide bound to latent and cleaved relative to native antithrombin can be explained by the locations of the four tryptophans, Trp49, Tr189, Trp225, and Trp307 (*42*). Trp225 at the end of the third strand of β-sheet A and Trp307 on helix H contribute most to the pentasaccharide-induced fluorescence change of native antithrombin (*42*), followed by Trp189 on helix F and Trp49 on the A-helix, close to the heparin-binding site. Superimposing the crystal structures of pentasaccharide-bound (1e05L) and free (1e03L) latent antithrombin showed that the position of Trp49 was most affected by pentasaccharide binding, followed by Trp189, whereas Trp225 and Trp307 were similarly positioned in the bound and free states. The lower florescence change observed for pentasaccharide binding to latent than to native antithrombin thus supports the conclusion that the conformational change in latent antithrombin occurs only at or around the pentasaccharide-binding site. The similar affinity, kinetics, and changes in tryptophan fluorescence observed for the binding of the normal pentasaccharide to cleaved as to latent antithrombin indicate that the pentasaccharide-induced conformational changes are similar for these antithrombin forms. Differences in changes in TNS fluorescence induced by pentasaccharide binding to latent as compared to cleaved

antithrombin are presumably due to TNS binding differently to these antithrombin forms. The finding that the normal pentasaccharide and high-affinity heparin, but not low-affinity heparin, caused a change in TNS fluorescence with latent and cleaved antithrombin suggests that the change in TNS fluorescence, like the tryptophan fluorescence change, reports the conformational change.

The similar fluorescence changes and affinities observed for HAH as for the normal pentasaccharide interacting with latent and cleaved antithrombin indicate that HAH binds to these antithrombin forms through the same pentasaccharide sequence that binds to native antithrombin. Moreover, the lack of fluorescence changes and the low affinities for the interactions of LAH with latent and cleaved antithrombin also support a specificity of latent and cleaved antithrombin for the pentasaccharide sequence, found only in HAH. LAH preparations are reported to have highly similar structures as HAH with the important difference that LAH lacks the 3-O-S group in unit F of the anticoagulant pentasaccharide sequence (*43, 44*). This 3-O-S group thus appears to enhance the affinity not only for native but also for latent and cleaved antithrombin. The 20- and 100-fold tighter binding of the high-affinity than of the normal pentasaccharide to latent and cleaved antithrombin, respectively, indicates that the addition of a 3-O-S group in unit H further enhances the affinity for latent and cleaved antithrombin. This finding is supported by a previous study using a structurally different high-affinity pentasaccharide that also contains a 3-O-S group in unit H (*8*), although it should be noted that both of these high-affinity pentasaccharides contain additional structural differences from the normal pentasaccharide that are not believed to be important for antithrombin binding. The higher affinities of the normal pentasaccharide than HAH for latent and cleaved antithrombin, although HAH contains this pentasaccharide sequence, demonstrate that the residues outside the pentasaccharide sequence of HAH that are attracted by native antithrombin (*30*) are repelled by latent and cleaved antithrombin. The glycan at Asn135 may contribute to this repulsive effect, as it also may do in the first step of binding of HAH to native antithrombin (*30, 34*). Alternatively, the repulsive effect could be due to acidic residues outside the pentasaccharide-binding site of latent and cleaved antithrombin. In either case, it is likely to occur toward the upper pole of the serpin (in a classical serpin orientation).

The findings presented in this work suggest that the pentasaccharide sequence may be a common site in heparin for mediating both anticoagulant activities of native antithrombin and antiangiogenic activities of latent and cleaved antithrombin forms. The restriction of antiangiogenic properties to latent, cleaved, and prelatent antithrombin forms is thus presumably caused by these variants expressing an antiangiogenic epitope which is hidden in native antithrombin but becomes exposed in loop-inserted forms, as proposed previously for prelatent antithrombin (*5*). This epitope is required for antithrombin to bind to a specific endothelial cell receptor and heparan sulfate coreceptor and thereby mediate antithrombin's antiangiogenic function (*8*). The suggestion that anticoagulant heparan sulfates also mediate FGF−FGFR interactions (*45*) suggests that the specific binding of antiangiogenic antithrombin to anticoagulant heparan sulfate may serve not only to promote binding to a specific receptor but also to antagonize growth factor−receptor interactions. Future studies will be required to verify such a mechanism.

ACKNOWLEDGMENT

The authors thank Professor Ingemar Björk for helpful comments and critical reading of the manuscript.

REFERENCES

1. O'Reilly, M. S., Pirie-Shepherd, S., Lane, W. S., and Folkman, J. (1999) Antiangiogenic activity of the cleaved conformation of the serpin antithrombin. *Science 285*, 1926–1928.
2. Larsson, H., Sjoblom, T., Dixelius, J., Ostman, A., Ylinenjarvi, K., Björk, I., and Claesson-Welsh, L. (2000) Antiangiogenic effects of latent antithrombin through perturbed cell-matrix interactions and apoptosis of endothelial cells. *Cancer Res. 60*, 6723–6729.
3. Larsson, H., Akerud, P., Nordling, K., Raub-Segall, E., Claesson-Welsh, L., and Björk, I. (2001) A novel anti-angiogenic form of antithrombin with retained proteinase binding ability and heparin affinity. *J. Biol. Chem. 276*, 11996–12002.
4. Zhang, W., Chuang, Y. J., Swanson, R., Li, J., Seo, K., Leung, L., Lau, L. F., and Olson, S. T. (2004) Antiangiogenic antithrombin down-regulates the expression of the proangiogenic heparan sulfate proteoglycan, perlecan, in endothelial cells. *Blood 103*, 1185–1191.
5. Richard, B., Swanson, R., Schedin-Weiss, S., Ramirez, B., Izaguirre, G., Gettins, P. G., and Olson, S. T. (2008) Characterization of the conformational alterations, reduced anticoagulant activity, and enhanced antiangiogenic activity of prelatent antithrombin. *J. Biol. Chem. 283*, 14417–14429.
6. Wardell, M. R., Chang, W. S., Bruce, D., Skinner, R., Lesk, A. M., and Carrell, R. W. (1997) Preparative induction and characterization of L-antithrombin: a structural homologue of latent plasminogen activator inhibitor-1. *Biochemistry 36*, 13133–13142.
7. Björk, I., and Fish, W. W. (1982) Production in vitro and properties of a modified form of bovine antithrombin, cleaved at the active site by thrombin. *J. Biol. Chem. 257*, 9487–9493.
8. Zhang, W., Swanson, R., Izaguirre, G., Xiong, Y., Lau, L. F., and Olson, S. T. (2005) The heparin-binding site of antithrombin is crucial for antiangiogenic activity. *Blood 106*, 1621–1628.
9. Zhang, W., Chuang, Y. J., Jin, T., Swanson, R., Xiong, Y., Leung, L., and Olson, S. T. (2006) Antiangiogenic antithrombin induces global changes in the gene expression profile of endothelial cells. *Cancer Res. 66*, 5047–5055.
10. Olson, S. T., and Chuang, Y. J. (2002) Heparin activates antithrombin anticoagulant function by generating new interaction sites (exosites) for blood clotting proteinases. *Trends Cardiovasc. Med. 12*, 331–338.
11. Petitou, M., Casu, B., and Lindahl, U. (2003) 1976−1983, a critical period in the history of heparin: the discovery of the antithrombin binding site. *Biochimie 85*, 83–89.
12. Nordenman, B., Danielsson, Å., and Björk, I. (1978) The binding of low-affinity and high-affinity heparin to antithrombin. Fluorescence studies. *Eur. J. Biochem. 90*, 1–6.
13. Rickles, F. R. (2006) Mechanisms of cancer-induced thrombosis in cancer. *Pathophysiol. Haemostasis Thromb. 35*, 103–110.
14. Peterson, C. B., and Blackburn, M. N. (1985) Isolation and characterization of an antithrombin III variant with reduced carbohydrate content and enhanced heparin binding. *J. Biol. Chem. 260*, 610–615.
15. Picard, V., Ersdal-Badju, E., and Bock, S. C. (1995) Partial glycosylation of antithrombin III asparagine-135 is caused by the serine in the third position of its N-glycosylation consensus sequence and is responsible for production of the beta-antithrombin III isoform with enhanced heparin affinity. *Biochemistry 34*, 8433–8440.
16. Olson, S. T., Björk, I., and Shore, J. D. (1993) Kinetic characterization of heparin-catalyzed and uncatalyzed inhibition of blood coagulation proteinases by antithrombin. *Methods Enzymol. 222*, 525–559.
17. Chang, W. S., Wardell, M. R., Lomas, D. A., and Carrell, R. W. (1996) Probing serpin reactive-loop conformations by proteolytic cleavage. *Biochem. J. 314* (Part 2), 647–653.
18. Arocas, V., Bock, S. C., Raja, S., Olson, S. T., and Björk, I. (2001) Lysine 114 of antithrombin is of crucial importance for the affinity

and kinetics of heparin pentasaccharide binding. *J. Biol. Chem. 276*, 43809–43817.
19. Zhou, A., Huntington, J. A., and Carrell, R. W. (1999) Formation of the antithrombin heterodimer in vivo and the onset of thrombosis. *Blood 94*, 3388–3396.
20. Olson, S. T. (1985) Heparin and ionic strength-dependent conversion of antithrombin III from an inhibitor to a substrate of alpha-thrombin. *J. Biol. Chem. 260*, 10153–10160.
21. Nordenman, B., Nystrom, C., and Björk, I. (1977) The size and shape of human and bovine antithrombin III. *Eur. J. Biochem. 78*, 195–203.
22. Petitou, M., and van Boeckel, C. A. (2004) A synthetic antithrombin III binding pentasaccharide is now a drug! What comes next? *Angew. Chem., Int. Ed. Engl. 43*, 3118–3133.
23. Meagher, J. L., Olson, S. T., and Gettins, P. G. (2000) Critical role of the linker region between helix D and strand 2A in heparin activation of antithrombin. *J. Biol. Chem. 275*, 2698–2704.
24. Olson, S. T., and Björk, I. (1991) Predominant contribution of surface approximation to the mechanism of heparin acceleration of the antithrombin-thrombin reaction. Elucidation from salt concentration effects. *J. Biol. Chem. 266*, 6353–6364.
25. Schedin-Weiss, S., Desai, U. R., Bock, S. C., Gettins, P. G., Olson, S. T., and Björk, I. (2002) Importance of lysine 125 for heparin binding and activation of antithrombin. *Biochemistry 41*, 4779–4788.
26. Olson, S. T., Bock, P. E., and Sheffer, R. (1991) Quantitative evaluation of solution equilibrium binding interactions by affinity partitioning: application to specific and nonspecific protein-heparin interactions. *Arch. Biochem. Biophys. 286*, 533–545.
27. O'Keeffe, D., Olson, S. T., Gasiunas, N., Gallagher, J., Baglin, T. P., and Huntington, J. A. (2004) The heparin binding properties of heparin cofactor II suggest an antithrombin-like activation mechanism. *J. Biol. Chem. 279*, 50267–50273.
28. Streusand, V. J., Björk, I., Gettins, P. G., Petitou, M., and Olson, S. T. (1995) Mechanism of acceleration of antithrombin-proteinase reactions by low affinity heparin. Role of the antithrombin binding pentasaccharide in heparin rate enhancement. *J. Biol. Chem. 270*, 9043–9051.
29. Nordenman, B., and Björk, I. (1978) Binding of low-affinity and high-affinity heparin to antithrombin. Ultraviolet difference spectroscopy and circular dichroism studies. *Biochemistry 17*, 3339–3344.
30. Olson, S. T., Björk, I., Sheffer, R., Craig, P. A., Shore, J. D., and Choay, J. (1992) Role of the antithrombin-binding pentasaccharide in heparin acceleration of antithrombin-proteinase reactions. Resolution of the antithrombin conformational change contribution to heparin rate enhancement. *J. Biol. Chem. 267*, 12528–12538.
31. Olson, S. T., Swanson, R., Raub-Segall, E., Bedsted, T., Sadri, M., Petitou, M., Herault, J. P., Herbert, J. M., and Björk, I. (2004) Accelerating ability of synthetic oligosaccharides on antithrombin inhibition of proteinases of the clotting and fibrinolytic systems. Comparison with heparin and low-molecular-weight heparin. *Thromb. Haemostasis 92*, 929–939.
32. Skinner, R., Chang, W. S., Jin, L., Pei, X., Huntington, J. A., Abrahams, J. P., Carrell, R. W., and Lomas, D. A. (1998) Implications for function and therapy of a 2.9 Å structure of binary-complexed antithrombin. *J. Mol. Biol. 283*, 9–14.
33. Record, M. T., Jr., Lohman, M. L., and De Haseth, P. (1976) Ion effects on ligand-nucleic acid interactions. *J. Mol. Biol. 107*, 145–158.
34. Turk, B., Brieditis, I., Bock, S. C., Olson, S. T., and Björk, I. (1997) The oligosaccharide side chain on Asn-135 of alpha-antithrombin, absent in beta-antithrombin, decreases the heparin affinity of the inhibitor by affecting the heparin-induced conformational change. *Biochemistry 36*, 6682–6691.
35. Hjelm, R., and Schedin-Weiss, S. (2007) High affinity interaction between a synthetic, highly negatively charged pentasaccharide and alpha- or beta-antithrombin is predominantly due to nonionic interactions. *Biochemistry 46*, 3378–3384.
36. Olson, S. T., Srinivasan, K. R., Björk, I., and Shore, J. D. (1981) Binding of high affinity heparin to antithrombin III. Stopped flow kinetic studies of the binding interaction. *J. Biol. Chem. 256*, 11073–11079.
37. Danielsson, Å., and Björk, I. (1978) The binding of low-affinity and high-affinity heparin to antithrombin. Competition for the same binding site on the protein. *Eur. J. Biochem. 90*, 7–12.
38. Jin, L., Abrahams, J. P., Skinner, R., Petitou, M., Pike, R. N., and Carrell, R. W. (1997) The anticoagulant activation of antithrombin by heparin. *Proc. Natl. Acad. Sci. U.S.A. 94*, 14683–14688.
39. Johnson, D. J., Li, W., Adams, T. E., and Huntington, J. A. (2006) Antithrombin-S195A factor Xa-heparin structure reveals the allosteric mechanism of antithrombin activation. *EMBO J. 25*, 2029–2037.
40. Belzar, K. J., Zhou, A., Carrell, R. W., Gettins, P. G., and Huntington, J. A. (2002) Helix D elongation and allosteric activation of antithrombin. *J. Biol. Chem. 277*, 8551–8558.
41. dela Cruz, R. G., Jairajpuri, M. A., and Bock, S. C. (2006) Disruption of a tight cluster surrounding tyrosine 131 in the native conformation of antithrombin III activates it for factor Xa inhibition. *J. Biol. Chem. 281*, 31668–31676.
42. Meagher, J. L., Beechem, J. M., Olson, S. T., and Gettins, P. G. (1998) Deconvolution of the fluorescence emission spectrum of human antithrombin and identification of the tryptophan residues that are responsive to heparin binding. *J. Biol. Chem. 273*, 23283–23289.
43. Kusche, M., Backstrom, G., Riesenfeld, J., Petitou, M., Choay, J., and Lindahl, U. (1988) Biosynthesis of heparin. O-sulfation of the antithrombin-binding region. *J. Biol. Chem. 263*, 15474–15484.
44. Razi, N., and Lindahl, U. (1995) Biosynthesis of heparin/heparan sulfate. The D-glucosaminyl 3-O-sulfotransferase reaction: target and inhibitor saccharides. *J. Biol. Chem. 270*, 11267–11275.
45. McKeehan, W. L., Wu, X., and Kan, M. (1999) Requirement for anticoagulant heparan sulfate in the fibroblast growth factor receptor complex. *J. Biol. Chem. 274*, 21511–21514.

BI801656U